Proton Structure Functions from HERA
- Low x to High Q^2 -
and Extracted Parton Densities

Stefan Riess
E-mail address: riess@mail.desy.de
II.Inst. für Experimentalphysik
Universität Hamburg, Germany
on behalf
of the H1 and ZEUS collaborations

Recent results from measurements of neutral and charged current double differential cross sections at HERA are presented. From the neutral current data the structure function F_2 is extracted. Within the framework of perturbative QCD (pQCD) these structure functions are analyzed. The range of applicability of pQCD reaches down to $Q^2 = 1$ GeV^2. The longitudinal structure function F_L is deduced from cross section measurements at large y and its magnitude is compatible with pQCD predictions. The measured heavy quark structure function for charm quarks is described by pQCD on the basis of boson gluon fusion process. Generally a good and consistent description of the data by pQCD is found.

1 Introduction

Deep inelastic scattering was and still is the best tool to unravel the structure of the nucleons. A recent review on the subject including first HERA data is given in [1]. This report summarizes the recent results until summer 1998. HERA as the first collider to accelerate and store a hadron and a lepton beam, has a center of mass energy of $\sqrt{s} = 300$ GeV that allows the exploration of the proton structure in beforehand untested kinematical regions. In the past years HERA collided 27.6 GeV positrons with 820 GeV protons. Two multi purpose detectors H1 and ZEUS were operated to measure the particles emerging from an interaction. Their performance is described elsewhere [3, 4].

2 Theoretical Overview

Neutral Current (NC) cross sections are measured over a large range in kinematics at HERA. The four momentum transfer $Q^2 = s \cdot x \cdot y$ is proportional to the product of Bjorken x and y, the inelasticity parameter, both x and y can vary between zero and unity. The Heisenberg uncertainty principle allows to interpret Q^2 as a resolution parameter. Down to $Q^2 \approx m_p^2 \approx 1$ GeV^2 partons of the proton are resolvable, below the quark parton model is not appropriate any more. The measurement performed at low Q^2 is thus important to see the range of validity of perturbative QCD. The measurement for $Q^2 \geq 3$ GeV^2 and large y makes the cross section sensitive to the longitudinal structure function F_L, a true next to leading order (NLO) effect. Assuming one boson exchange for the description of the process depicted in fig.1 the Born cross section can be written as:

$$\frac{d^2\sigma}{dxdQ^2} = \frac{2\pi\alpha^2}{xQ^4}\left[Y_+F_2(x,Q^2) - Y_- xF_3(x,Q^2) - y^2F_L(x,Q^2)\right], \qquad (1)$$

here $Y_\pm = 1 \pm (1-y)^2$ is a kinematical factor. In leading order (LO) the structure

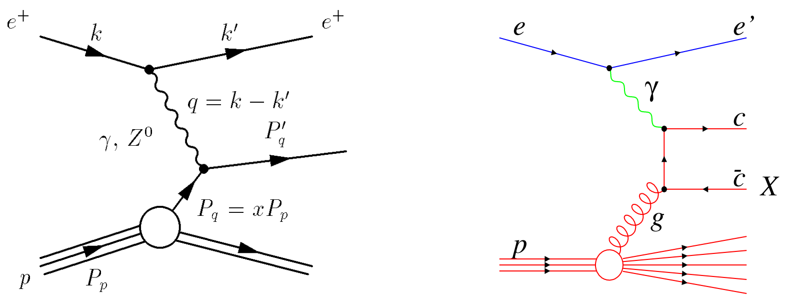

Fig. 1: Left: Quark parton model Feynman diagram for the interaction of a virtual boson with a parton of the proton. Right: Boson Gluon Fusion diagram representing a higher order effect, which is the basis for the calculation of the charm structure function F_2^c.

function F_2 is just the sum of all quark densities weighted with their charges squared. For the graphical presentations within this report the kinematical prefactor $\kappa = \frac{2\pi\alpha^2}{xQ^4}Y_+$ has been taken out from all cross sections.

At large $Q^2 \geq 6000$ the resolution or equivalently lifetime is sufficiently small to feel the influence of heavy light, namely the Z^o–boson. The NC cross section gets therefore additional contributions from pure Z^o exchange and the γ-Z^o–interference. The reader is referred to [5] for the detailed notation. The sensitivity to electroweak effects is discussed in the contribution of N.Brümmer to this conference [2]. For $Q^2 \geq 400$ the first double differential charged current (CC) cross sections for x and Q^2 have been measured at HERA.

The longitudinal structure function F_L has an impact on the cross section only at high y due to its kinematical prefactor. It vanishes in leading order and is therefore a true higher order effect.

The production of heavy quark flavors in the final state like charm is described in NLO pQCD by Boson gluon fusion (BGF) which is depicted in fig.1 (right) the corresponding structure function is called F_2^c and is strongly related to the gluon density [6]. The BGF process is a good approximation for cross section calculation when $Q^2 \approx m_c^2$. A generalized descriptions for all Q^2 were proposed by two different groups [7, 8].

Perturbative QCD (pQCD) is used for the prediction of Q^2 evolution of parton densities and therefore structure functions as well. The theoretical framework is reviewed in the contribution of J.Kwiecinski to this conference [9]. The evolution is governed by gluon emission from the quarks and the splitting of a gluon into a quark anti quark pair.

The shape of F_2 in x, which is of non perturbative origin cannot be predicted by pQCD. It is therefore modeled:

$$q(x) = A \cdot x^b \cdot (1-x)^c \cdot (1 + d \cdot x + e \cdot \sqrt{x}) \tag{2}$$

q stands for valence quarks u and d, the gluon density g and the sea quark density S. The normalization A is fixed by quark number counting rules for the valence quarks and the gluon by total momentum conservation. The term x^b is inspired by Regge phenomenology [9] and determines the structure function behavior at low x; parameter c is determined by the number of spectator quarks in the nucleon.The polynomial is purely phenomenological. These parameters are fitted in a global fit to the F_2 data at an initial reference scale Q_o^2. The fit includes as well the QCD scale parameter Λ, that determines the strong coupling constant α_s and therefore the Q^2 evolution. The gluon density determined in such a global fit is then in turn used to predict F_L and F_2^c and gives a consistency test of pQCD using HERA data only.

3 Experimental Results

F_2 is found to grow monotonically with decreasing x for all Q^2 measured so far. This growth is damped when Q^2 gets smaller. In fig. 2 the F_2 data from H1 [10] are shown together with results from fixed target experiments [11, 12, 13] over a huge range in kinematics. Q^2 and x span 5 orders of magnitude. The solid line represents a NLO pQCD fit to all these data and demonstrates how well these data can be described by the theory. The variation of F_2 with Q^2, scaling violations, are negative for $x \geq 0.1$ and positive below. It is understood as caused by soft gluon emission that shuffles proton momentum from large to low x. These gluons drive the sea quark density and therefore F_2 at low x, which leads to an F_2 that grows with increasing Q^2 at low x.

The ZEUS collaboration has studied the transition region [14] where $Q^2 \approx m_{proton}$. F_2 data with $Q^2 < 7$ GeV^2 is shown in fig.3. F_2 rises with decreasing x for all Q^2 but the x dependence gets rather weak at $Q^2 \leq 0.3$ GeV^2. Furthermore the prediction from their NLO pQCD fit for these data is shown. The fit defined the parameterizations (eq. 2) at $Q_o^2 = 7$ GeV^2. Using backward evolution the comparison between data and F_2 prediction shows that around $Q^2 \sim 1$ GeV^2 the description by pQCD starts to fail. Starting from the low Q^2 the data is successfully described by means of a Regge fit which is shown by the dashed line in fig.3. This non perturbative approach fails for $Q^2 \sim 1$ GeV^2 as well to describe the data. Therefore this is a very important region to study QCD and the variety of theoretical concepts is discussed for this conference in [9].

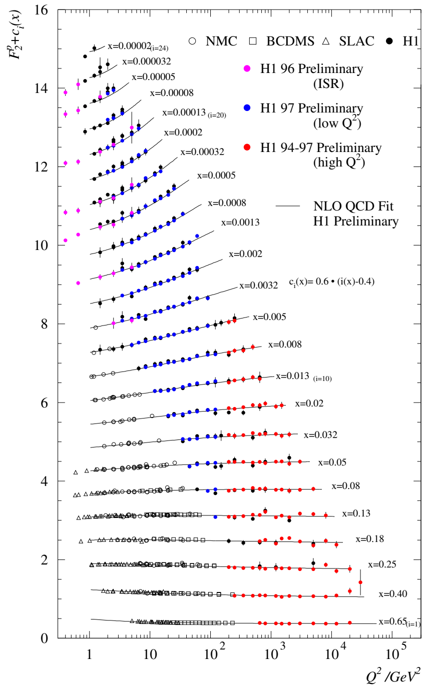

Fig. 2: F_2 from proton targets in the range of $Q^2 \approx 1$ to 30000 GeV^2, and for x values between .00002 and 0.65, assuming xF_3 and F_L as given by the Standard Model. The result of a pQCD fit is given by the sold lines. The data is scaled up by the factor given above for display only. The error bars represent the total error of the measurements.

Gluon Density

A NLO pQCD fit to F_2 data determines the gluon density. Within the analyzes the experimental systematic errors have been propagated. That leads to an error band for the resulting gluon, which is shown in fig.4 at $Q^2 = 20$ GeV^2. The results of fits to HERA data by H1 and ZEUS are in good agreement with each other. The large x domain is covered by a similar analysis of fixed target data by NMC [11]. The gluon densities obtained in global fits to all data that can constrain parton densities are in good agreement with the results from the collaborations. The outdated GRV-94HO gluon density has too much glue at low x in comparison to the fits done by the collaborations; but is still used as a reference within other figures shown in this report. The gluon density from pQCD fits will further be used for the prediction of F_2^c and F_L.

Longitudinal Structure Function

Measurement of the cross section at large y allows the study of the influence of F_L on the cross section. At large y the energy of the scattered electron is small $E \sim 6$ GeV and the background from photoproduction has to be controlled rather careful. A true measurement would need different center of mass energies in order to determine the

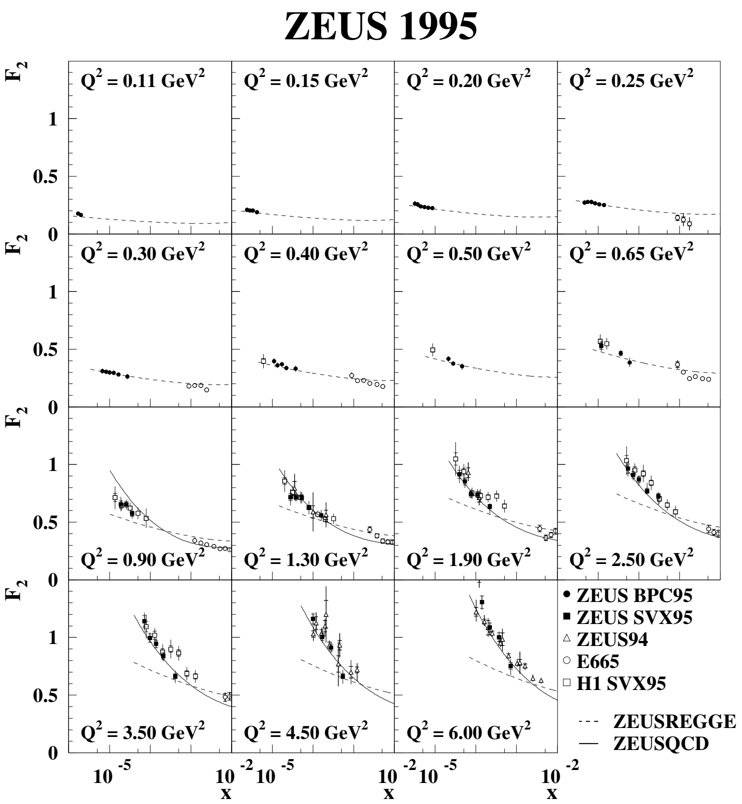

Fig. 3: Very low Q^2 F_2 data in comparison with a Regge model fit (dashes line) and the prediction of F_2 from a NLO pQCD fit to data with $Q^2 \geq 7$ GeV^2.

y dependence for constant x and Q^2. The H1 collaboration has two methods for F_L extraction from the cross section. The subtraction method [15], where F_L is given by the difference between the measured cross section and the cross section using only the F_2 predicted from pQCD fits $\frac{y^2}{Y_+}F_L = F_2^{fit} - \frac{1}{\kappa}\frac{d^2\sigma^{exp}}{dxdQ^2}$. These fits use in turn only data points with $y < 0.6$ thus being independent from F_L [15]. A recently proposed method [16] measures the logarithmic scaling violations with y of the cross section.

$$\frac{d\tilde{\sigma}}{dlog(y)} = \frac{dF_2}{dlogx} + \frac{dF_L}{dlogx}\frac{y^2}{Y_+} - 2y^2\frac{2-y}{Y_+}F_L \qquad (3)$$

This cross section is shown in fig.5 the solid line is the outcome from a pQCD fit from which F_L is calculated, for the dotted line $F_L = F_2$ is assumed and the dashed line represents $F_L = 0$. It is obvious that in all Q^2 bins a contribution from F_L is needed at large y and that its magnitude is consistently described by a NLO pQCD fit. The results for the extracted F_L are in good agreement between the two methods [16].

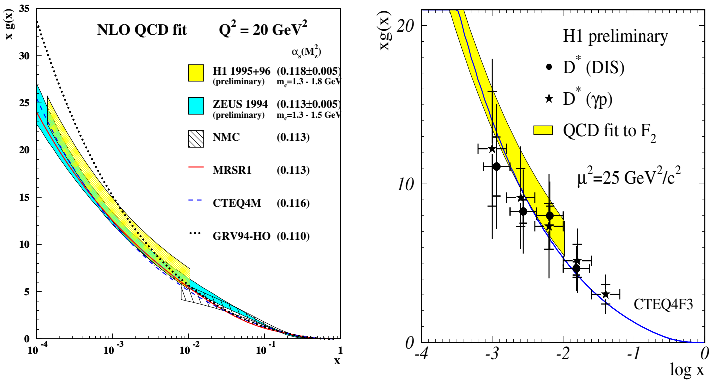

Fig. 4: Left: Gluon density $xg(x)$ from H1, ZEUS and NMC at $Q^2 = 20$ GeV^2 as function of x. Right: Gluon density extracted from the charm structure function F_2^c.

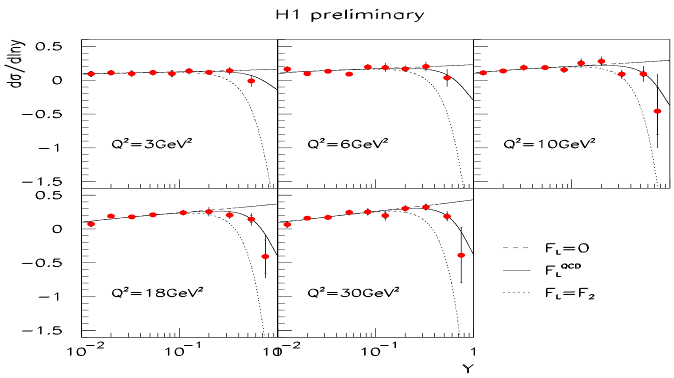

Fig. 5: Measurement of the derivative $d\sigma/dlog(y)$. The curves represent the QCD cross section fit including F_L (solid line), neglecting it (dashed line) and setting $F_L = F_2$ (dotted line).

Heavy Quarks – $\mathbf{F_2^c}$

A crucial test for NLO pQCD calculations is given by heavy quark structure function. This is caused by the heavy quark mass that sets another hard scale besides Q^2. The basic diagram for the boson–gluon–fusion process was shown in fig.1 (right) and shows that the prediction of F_2^c is related to the gluon density. Experimentally the charm content of the proton can be measured by tagging events in which a $D^{*+} \rightarrow (D^o \rightarrow K^-\pi^+)\pi^+$ or charge conjugate is produced. The reconstruction of the D–mesons is feasible in a limit rapidity range $|\eta(D^{*\pm})| < 1.5$ and for transverse momenta $1.5 <$

$p_T(D^{*\pm}) < 15$ GeV. The total production cross section for $0.02 < y < 0.7$ and $1 < Q^2 < 600$ GeV^2 is measured by the ZEUS collaboration to be $\sigma_{charm} = 8.55 \pm 0.31^{+0.30}_{-0.50}$ nb [17]. Extrapolation over the full phase space in η and p_T yields the charm production cross section: $\frac{d^2\sigma_{c\bar{c}X}}{dx\, dQ^2} = \frac{2\pi\alpha^2}{xQ^4}[1 + (1-y)^2 F_2^c(x,Q^2)]$, from which F_2^c is extracted. Fig.6 shows the x dependence of F_2^c in bins Q^2. Similar strong rise with decreasing x is observed as for the inclusive F_2. The analysis furthermore shows that F_2^c contributes 10% to the total F_2 at smallest Q^2 and 30% for $Q^2 \geq 30$ GeV^2 [17]. These findings are consistent with the measurement of the same observable by H1 [18] The expectation using the parton densities from the global fit to F_2 is shown as solid line with the broken lines indicating the error band. The GRV-94HO [6] parton densities were used to study the influence of charm quark mass variation between 1.2–1.6 GeV the resulting range is given by the shaded error band. Within the experimental errors the theoretical description based on BGF process is satisfactory. The gluon density extracted from F_2^c is in good agreement with the gluon from the pQCD fits as shown on the right hand side of fig.4.

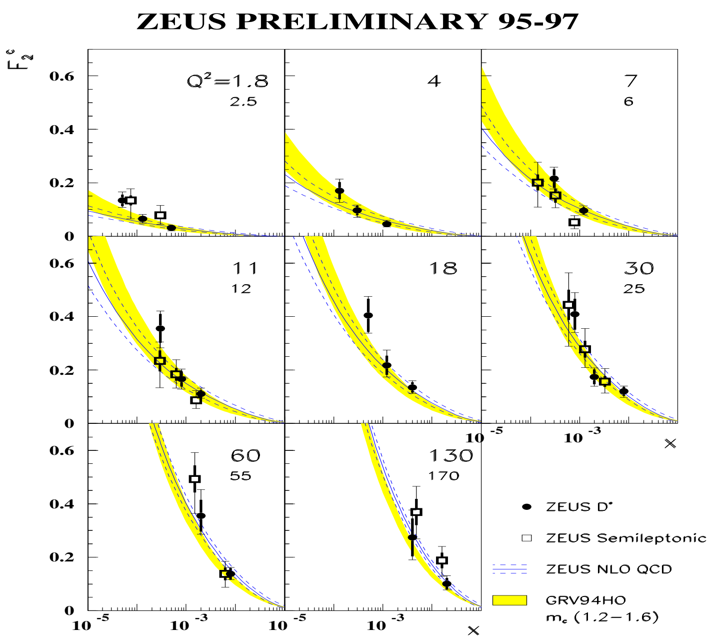

Fig. 6: The measured F_2^c at Q^2 between 1.8 and 130 GeV^2 as function of x. Inner error bars denote the statistical uncertainty and the outer ones the total uncertainty. The curves are explained in the text.

High Q^2

The large x and $Q^2 \geq 200$ GeV^2 samples comprise all data taken with positron beam. All experimental details are described in [19]. The H1 data ($\tilde{\sigma}$) and fixed target F_2 are shown in fig.7 for large x as a function of Q^2. Here $\tilde{\sigma} = 1/\kappa d^2\sigma/dx/dQ^2$ represents the structure function term, which below $Q^2 \leq 3000$ GeV^2 $\tilde{\sigma}$ is given by F_2. The presence of xF_3 yields another linear combination of quark densities for $\tilde{\sigma}$ than F_2. The solid lines represent the cross section $\tilde{\sigma}$ calculated from parton densities that were obtained without the new H1 data (MRST grey [20]) and a pQCD fit that included them (dark line) [19]. The drop of the cross section at highest Q^2 is caused by electroweak effects and discussed in [2]. Small differences are noticeable, thus the high x data from HERA eventually constrains future global pQCD fits. The Q^2 evolution, governed by the strong coupling constant, extends over almost four orders of magnitude and is described fairly well by pQCD. At $x = 0.45$ and $Q^2 > 10000$ GeV^2 some two standard deviations persist [2].

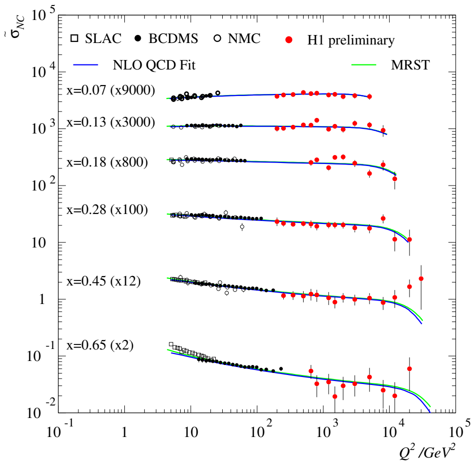

Fig. 7: Neutral current structure function term $\tilde{\sigma}$ data from H1 and fixed target experiments as function of Q^2 for various bins in x and $x \geq 0.07$. Curves show predictions using partons from various pQCD fits that are explained in the text.

HERA allows at large Q^2 also the study of the charged current process. The selection of these events is possible for minimum transverse momentum around 12 GeV resulting in a minimal $Q^2 \approx 200$ GeV^2. The first measurement of the double differential cross section at large Q^2 $\frac{d^2\sigma}{dx\,dQ^2}$ from HERA (H1 [19] and ZEUS [21]) yields structure function terms with very different linear combinations of quark flavors, because the charged current process is flavor sensitive caused by the helicity structure of the weak interaction. The structure function term for CC is obtained from the measured cross section, where the Fermi coupling constant G_F and the propagator term, discussed in [2], $(1+Q^2/m_W^2)^{-2}$ are taken out.

$$\sigma_{CC} \equiv \frac{2\pi x}{G_F^2} \frac{m_W^4}{(Q^2+m_W^2)^2} \frac{d^2\sigma}{dxdQ^2} = x(\bar{u}+\bar{c}+(1-y)^2(d+s)) \qquad (4)$$

Positron induced reactions are sensitive to the d-valence quark and $\bar{u}, d, s$ and $\bar{c}$–sea quarks. The measured x dependence of the structure function term [21] for various Q^2 bins are depicted in fig.8. The linear combinations of $d+s$ (dashed line) and $\bar{u}+\bar{c}$ (dotted line) and their sum (solid line) are indicated in fig.8 using parton densities taken from [22]. At high x the charged current positron induced process is dominated from scattering off valence d quarks. The inclusion of these data in global fits will

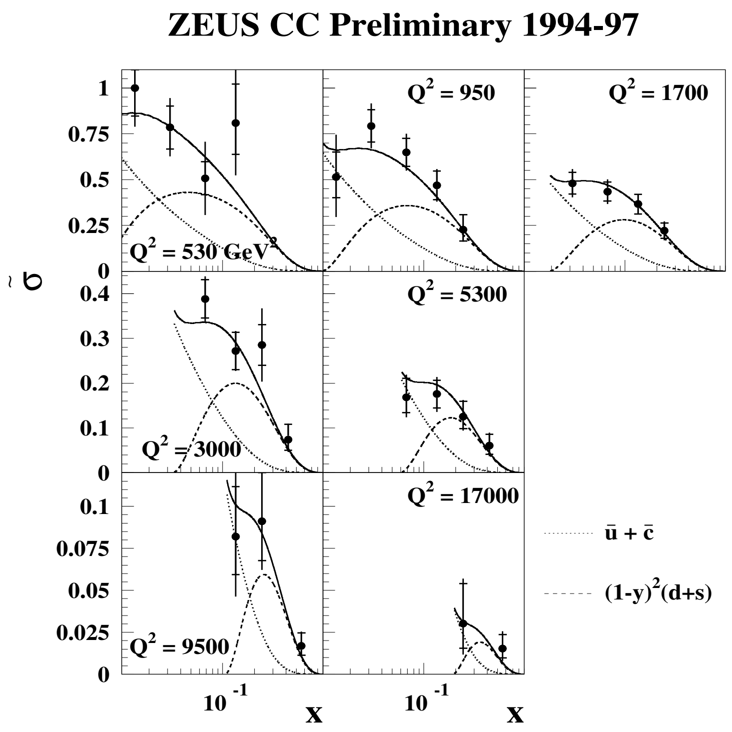

Fig. 8: Charged current structure function term data from ZEUS a function of x in bins of Q^2. The curves represent the prediction from CTEQ4D partons (solid line) and the contributions individually from quarks (dashed line) and from anti quarks (dotted line).

certainly improve the knowledge of parton densities, since these data provide different linear combinations of quark flavors.

4 Conclusion

The HERA experiments H1 and ZEUS have extended the kinematical region for the study of the proton structure quite extensively. The statistical precision is of order few per cent with small systematical errors. The cross section at low x and large y needs a contribution from the longitudinal structure function for a description by pQCD. The measurement of final states containing the heavy charm quark leads to the charm structure F_2^c. Its size and kinematical dependencies are well described by calculations on the basis of the boson gluon fusion process. Gluon densities extracted from perturbative QCD fits are in good agreement amongst the experiments. High x data probes the Q^2 evolution over four orders of magnitude and the HERA data extends the fixed target data in Q^2. Charged current double differential cross section that are flavor sensitive add information on proton structure. Further increase in statistics will help to clarify small discrepancies in the description of deep inelastic scattering cross sections by perturbative QCD. The wealth of the data can be described by means of pQCD with impressive precision.

Acknowledgment

I would like to thank the organizers for a very pleasant conference in Stara Lesna.

References

[1] A.M. Cooper-Sarkar, R.Devenish and A.DeRoeck: *Int.J.Mod.Phys.* **A13** (1998) 3385;
[2] N.Brümmer,: *contr. to these proceedings* (1998) ;
[3] I.Abt et al.: *NIM* **A386** (1997) 310;
I.Abt et al.: *NIM* **A386** (1997) 348;
[4] M.Derrick et al.: *The ZEUS detector, Status Report, DESY* (1993) ;
[5] R.Beyer et al.: *Future Physiccs at HERA* **1** (1996) page;
[6] M.Glück, E.Reya and A.Vogt: *Z.Phys.* **C67** (1995) 433;
[7] M.Aizvas et al.: *Phys.Rev.* **D50** (1994) 3085;
[8] R.Thorne and R.Roberts: *Phys.Lett.* **B421** (1998) 303;
[9] J.Kwieczinski,: *contr. to these proceedings* (1998) ;
[10] H1 collaboration: *Contribution to ICHEP98* **Abstract** (1998) ;
[11] M.Arneodo et al.: *Nucl. Phys.* **B483** (1997) 3;
[12] A.Benvenuti et al.: *Phys.Lett.* **B223** (1989) 485;
[13] L.Whitlow et al.: *Phys.Lett.* **B282** (1992) 475;
[14] ZEUS Collaboration: *DESY preprint* **121** (1998) ;
[15] S.Aid: *Phys.Lett* **B393** (1997) 452;
[16] H1 collaboration: *Contribution to ICHEP98* **Abstract 534** (1998) ;
[17] ZEUS collaboration: *Contribution to ICHEP98* **Abstract 768** (1998) ;
[18] H1 collaboration: *Contribution to ICHEP98* **Abstract 540** (1998) ;
[19] H1 collaboration: *Contribution to ICHEP98* **Abstract 533** (1998) ;
[20] A.Martin et al.: *DTP/98/10, RAL-TR-98-029* (1998) ;
[21] ZEUS collaboration: *Contribution to ICHEP98* **Abstract 751** (1998) ;
[22] H.Lai et al.: *Phys.Rev.* **D55** (1997) 1280;